JOURNAL OF ELECTROMAGNETIC ENGINEERING AND SCIENCE, VOL. 24, NO. 4, 393~400, JUL. 2024

https://doi.org/10.26866/jees.2024.4.r.239
ISSN 2671-7263 (Online) · ISSN 2671-7255 (Print)

# Design of an All-Metal Vivaldi Array Antenna with Dual-Slant Polarization for High-Power Jammer Systems

Tae Heung Lim[1] · Seulgi Park[2] · Cheol-Soo Lee[3] · Joo Rae Park[3] · Hosung Choo[4,*]

## Abstract

In this paper, we propose an all-metal Vivaldi array antenna with dual-slant polarization for high-power jammer systems. The single Vivaldi element of the proposed array consists of radiating flares and an inner cavity to achieve high directivity and wide-frequency band impedance-matching characteristics. We expanded the proposed Vivaldi element to a 4 × 4 array antenna with dual-slant polarization considering the occurrence of grating lobes. The fabricated array antenna produced measured active voltage standing wave ratios below 2.74:1 (Port 1) and 2.85:1 (Port 6) in the frequency range of 2.5–5.5 GHz for all steering angles. In addition, the measured array gain is above 9.5 dBi in the frequency range from 2 GHz to 6 GHz. These results confirm that the proposed array antenna consisting of metallic components for high durability is suitable for application to high-power jammers.

**Key Words**: Dual-Slant Array Antenna, High-Power Jammer, Metal Vivaldi Antenna.

## I. Introduction

In modern electronic warfare, dramatic advances in multifunctional radars, high-precision surveillance systems, and high-speed radio communications have led to increased interest in high-power jammers that can use radio frequency waves to interfere with or perturb other electronic systems. In high-power jammer systems, it is important to design a phased array antenna to have a broad bandwidth characteristic, because most recent military radio equipment adopts multifunctional performance across multiple frequency bands. Various studies have designed broadband array antennas with inexpensive printed circuit boards, such as Vivaldi antennas [1], log-periodic dipole antennas [2], and broadband monopole antennas [3, 4]. Although such antennas can have wide operating frequency bands, their large geometric sizes and low durability typically make them unsuitable for high-power jammer systems. To reduce the array aperture size, a number of miniaturized metallic broadband antennas with flared-notched [5, 6], cone [7], and horn [8] shapes have been introduced. However, a small array aperture size leads to a low array gain performance in high-power jamming applications. In addition, an in-depth study is needed to design an array antenna for high-power jammers based on beam-steering properties and array configurations.

In this paper, we propose an all-metal Vivaldi array antenna with dual-slant polarization for high-power jammer systems. The single Vivaldi element of the proposed array consists of radiating flares and an inner cavity, based on the model developed in [9]. The proposed array element needs a high array gain performance

Manuscript received July 03, 2023 ; Revised December 08, 2023 ; Accepted December 29, 2023. (ID No. 20230703-117J)
[1]School of Electronic Engineering, Kumoh National Institute of Technology, Gumi, Korea
[2]Hanwha Systems, Seongnam, Korea.
[3]Agency for Defense Development, Daejeon, Korea.
[4]Department of Electronic and Electrical Engineering, Hongik University, Seoul, Korea.
*Corresponding Author: Hosung Choo (e-mail: hschoo@hongik.ac.kr)

in the low-end frequency band for use in high-power jammer systems to maximize the width (the array distance) and increase the electrical aperture size. Furthermore, the width of the proposed array element is determined by considering the maximum beam-steering range with the occurrence of a grating lobe. The radiating flares are adjusted to obtain high directivity with minimized pattern distortion in the bore-sight direction. The inner cavity of the antenna has a significant impact on the impedance matching characteristics, allowing wideband operation. The detailed design parameters for the array element are optimized at the bore-sight direction based on an infinite periodic array to achieve broad frequency band characteristics. Considering grating lobes, we then expand the proposed Vivaldi element to a 4 × 4 array antenna with dual-slant polarizations. To confirm the feasibility of the proposed array antenna, we fabricated a prototype and conducted measurements in an anechoic chamber to evaluate its antenna properties, such as the active voltage standing wave ratio (AVSWR), active element pattern (AEP), array gain, and steered beam pattern. The results demonstrate that the proposed array antenna consisting of metallic components for high durability is suitable for application to high-power jammers due to its enhanced gain considering the steered beam performance.

## II. Proposed Antenna Design

### *1. Array Distance Determination Considering the Grating Lobe*

Fig. 1(a) and 1(b) show the planar and triangular array configurations of the Vivaldi antenna with slant polarization. For high-power jammer applications, the array antenna aperture needs to be as large as possible because the array requires high-gain properties. In addition, it is essential to determine the array distances ($dx_1$ and $dy_1$) and the total Vivaldi width ($w$) to avoid unwanted grating lobes for beam steering. In a uniform planar array, the array distances ($dx'_1 = dy'_1 = 42$ mm [0.84λ at 6 GHz]) along the $x$- and $y$-axes are equal. A grating lobe does not occur until the maximum steered beam at angles of $Az = 12.2°$ and $El = 11.9°$. However, it did not achieve the required beam-steering angles ($-45° \le Az \le 45°$ and $-25° \le El \le 25°$) in this research, as shown in Fig. 2(a). On the other hand, Fig. 2(b) presents the improved grating-lobe-free region of the triangular array, despite the array distance $dx_1$ being equal to that of the planar array. $dx_2$ ($x$-shifted array distance at an even-numbered row), and $dy_1$ are half of $dx_1$. These array distances result in an isosceles-right triangular array configuration that can increase the grating-lobe-free region up to the required beam steering region. Based on the results, the total Vivaldi width $w$ can be determined as 29.7 mm, which is the square root of $dx_1$.

### *2. Micro-Doppler Effect*

Fig. 3(a) and 3(b) illustrate the geometry of the proposed array element. The proposed Vivaldi element, based on Kindt's model [9], is composed of radiating flares and a cavity part. The radiating flares have exponential curves using a function of $f(z)$, as follows:

$$f(z) = ae^{\left(b(z-l_2)+\frac{w_3}{2a}-1\right)}, \tag{1}$$

$$b = \frac{\ln\left(\frac{w_1-w_3}{2a}+1\right)}{l_1}. \tag{2}$$

We determined the flare curves to achieve high directivity for high-power jammers. The length $l_1$ affects the number of resonances in the broadband frequency band. The cavity part is an important component of the proposed antenna geometry that can

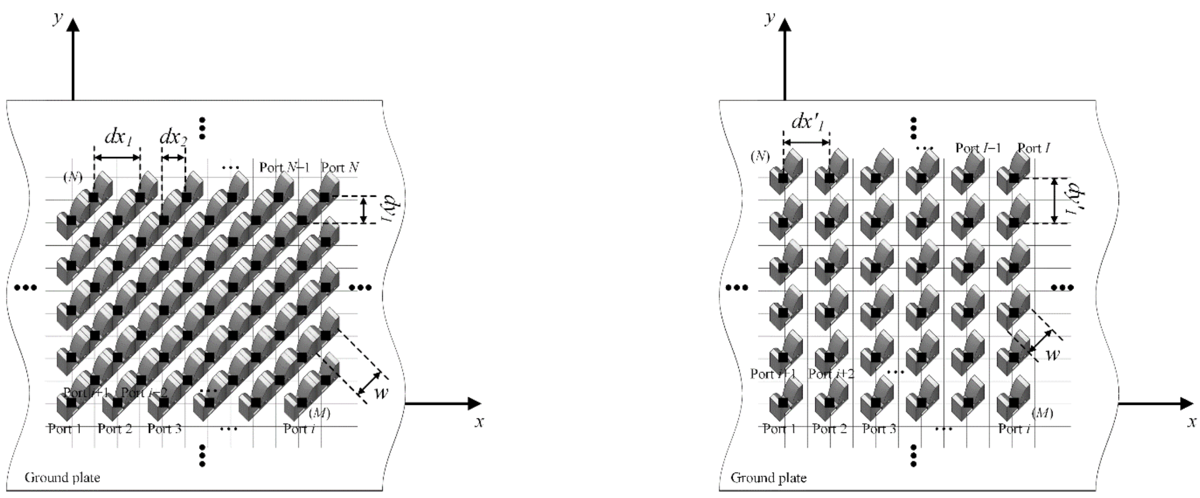


(a) (b)

Fig. 1. Geometries of array configuration: (a) planar array configuration and (b) triangular array configuration.

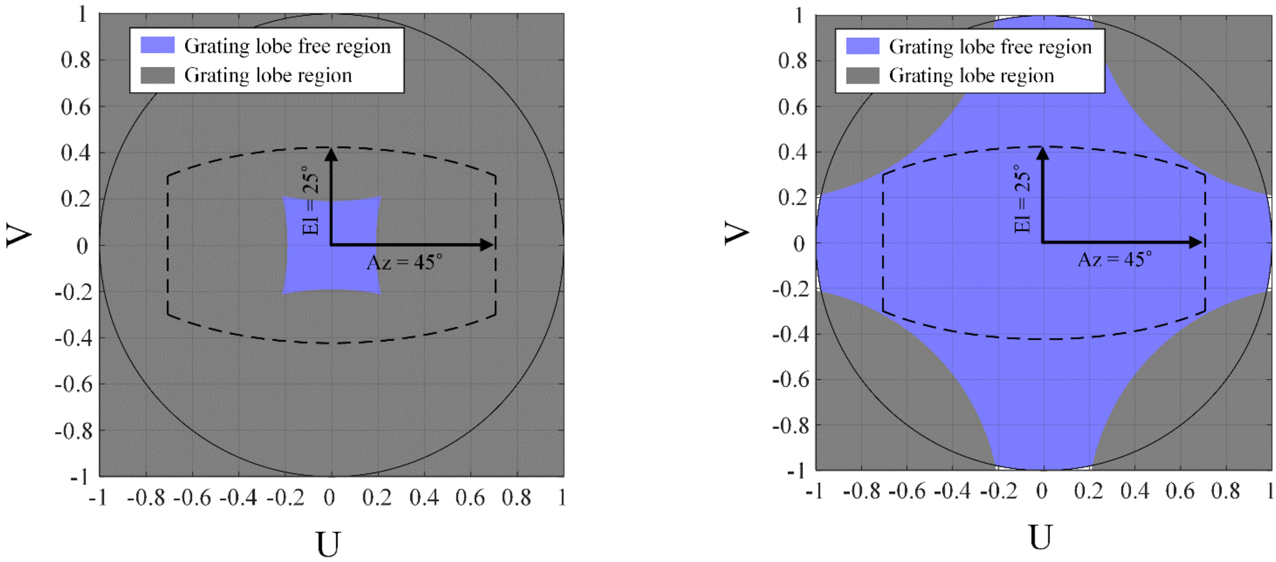


(a) (b)

Fig. 2. Grating-lobe-free region and grating lobe region: (a) planar array configuration and (b) triangular array configuration.

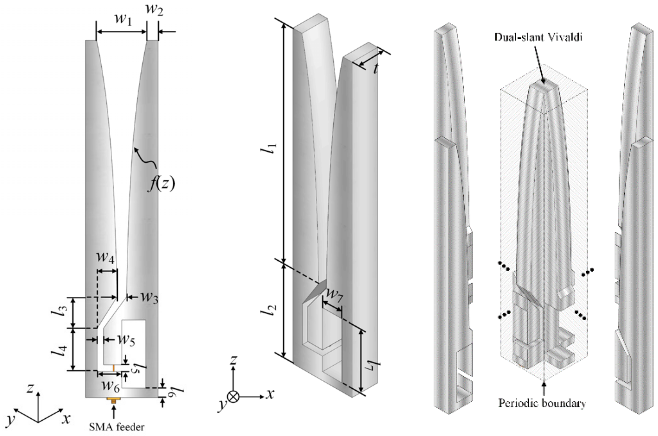


(a) (b) (c)

Fig. 3. Geometry of proposed array element: (a) front view, (b) isometric view, and (c) periodic structure.

improve the broadband impedance matching characteristics. The total area of the metal component for the proposed element can be adjusted according to the width $w_7$ and length $l_7$ of the rectangular cavity. It can tune the antenna port reflections in the low-end frequency band because the electrical current path lengthens when the metal area increases. Then, the cavity and the radiating flares are connected through linear transmission lines, which enable fine-tuning of the broadband impedance matching characteristics. Fig. 3(c) presents the extension of the periodic structure for observing the AVSWR in consideration of dual-slant polarization. Vivaldi array elements are rotated by ±45° and integrated so that their edge sides are shared. Herein, the width $w_2$ is half the Vivaldi thickness $t$. We then optimize the proposed array element parameters based on the infinite periodic array to achieve broad frequency band operation, and the detailed parameters are listed in Table 1. Fig. 4 shows the simulated AVSWRs of the periodic structure from 2–6 GHz at steering angles (*Az*, *El*) of (0°, 0°), (45°, 0°), and (0°, 25°). There is an abnormal peak near the central frequency band that can be adjusted by the parameters $t$ and $l_1$. In our research, the thickness should be maximized to enhance the array gain in the low-end frequency band, so that $t$ and $l_1$ are optimized by 10 mm and 56 mm, respectively. to achieve the maximum AVSWRs at steering angles (*Az*, *El*) of (0°, 0°) and (45°, 0°) below 3:1 over the operating frequency band.

## III. ARRAY FABRICATION AND MEASUREMENT

### *1. Array Expansion and Fabrication*

Fig. 5 represents the proposed array antenna having dual-slant polarization with 32 elements (a 4 × 4 triangular array configuration) for high-power jamming applications. To observe

Table 1. Optimized dimensions of the 1 × 4 array

| Parameter | Value | Parameter | Value |
|---|---|---|---|
| $w_1$ | 19.7 | $l_1$ | 166 |
| $w_2$ | 5 | $l_2$ | 56 |
| $w_3$ | 3.5 | $l_3$ | 21.6 |
| $w_4$ | 8.4 | $l_4$ | 14.7 |
| $w_5$ | 2.5 | $l_5$ | 1.5 |
| $w_6$ | 10.5 | $l_6$ | 4.7 |
| $w_7$ | 6.35 | $l_7$ | 34.4 |
| $a$ | 0.16084 | $t$ | 10 |

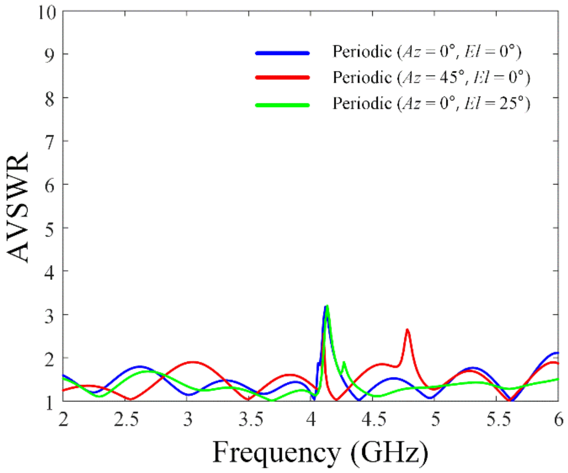


Fig. 4. AVSWR of the proposed periodic structure according to beam steering angles.

the array performance, the +45° slant-polarized elements are excited to obtain the *S*-parameter matrix and active element patterns, while the other polarized elements are terminated with 50-Ω loads. Fig. 6(a) shows each component of the proposed array antenna: radiators, a cavity part, a ground plate, and SMA feeders. In particular, the modularized radiating components can easily be replaced in case of breakdown or malfunction. Fig. 6(b) illustrates the assembly process employing bolts and nuts for high durability and easy fabrication. Fig. 6(c) and 6(d) show photographs of the fabricated array antenna.

*2. AVSWR Results*

To observe the AVSWRs of the proposed array, the +45° slant-polarized elements are measured using a two-port vector network analyzer. All ports are measured to obtain a 16 × 16 *S*-matrix for the AVSWR calculation according to the *Az* and *El* directions as follows [10–12]:

$$\Gamma_i(Az, El) = \sum_{n=1}^{N/2}\sum_{m=1}^{M} S_{i,m+M(n-1)}\left(e^{-jk[(m-1)dx_1u_0+(2n-2)dy_1v_0]} + e^{-jk[\{dx_2+(m-1)dx_1\}u_0+(2n-1)dy_1v_0]}\right), \quad (3)$$

$$u_0 = \sin(Az)\cos(El),\ v_0 = \sin(El), \quad (4)$$

$$AVSWR_I = \frac{1+|\Gamma_i(Az, El)|}{1-|\Gamma_i(Az, El)|}. \quad (5)$$

$\Gamma_i(Az, El)$ is the active reflection coefficient of the *i*-th port according to the steering angle in the azimuth and elevation directions, and *i* is the port index number ($i = 1, 2, \ldots, I$). *m* and

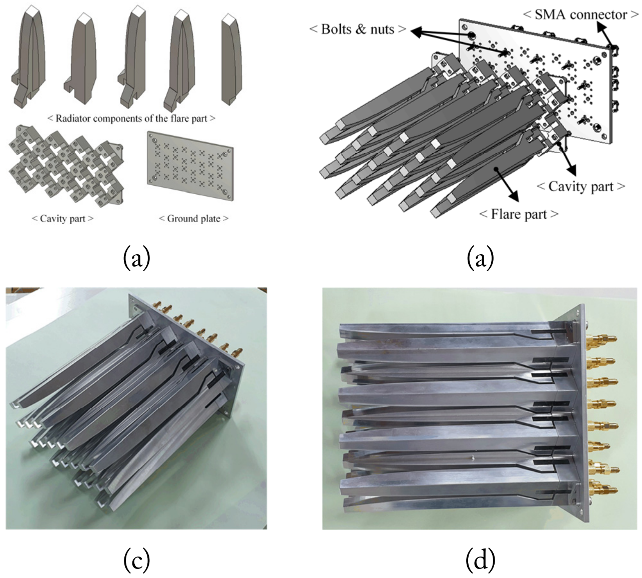


Fig. 6. Photographs of the fabricated array antenna: (a) partial components of the antenna parts for fabrication and (b) assembly fabrication process, and (c) isometric view and (d) side view.

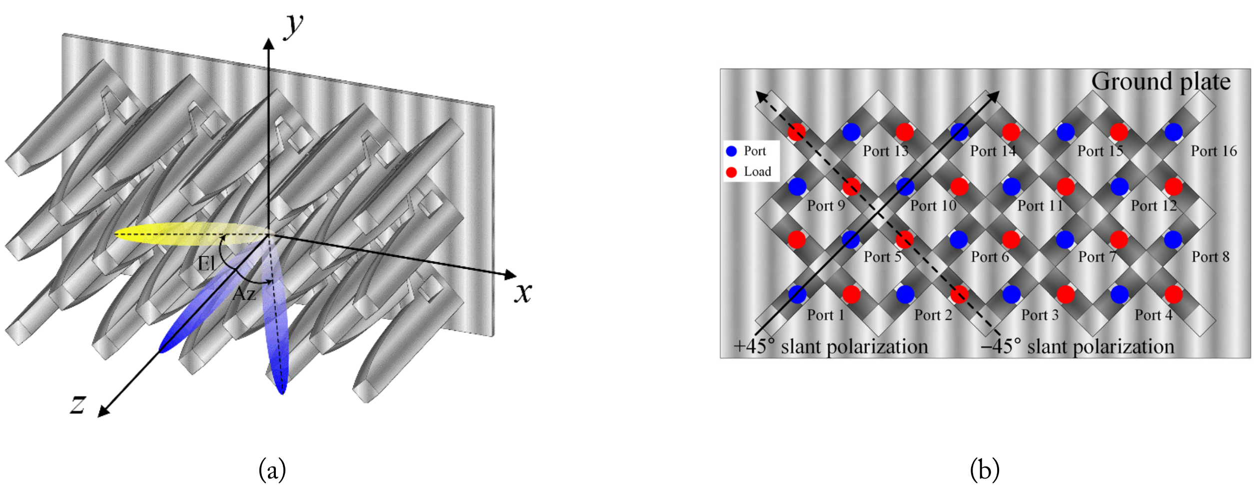


Fig. 5. The proposed array antenna, with dual-slant polarization and 32 elements in a 4 × 4 triangular array configuration: (a) isometric view and (b) top view.

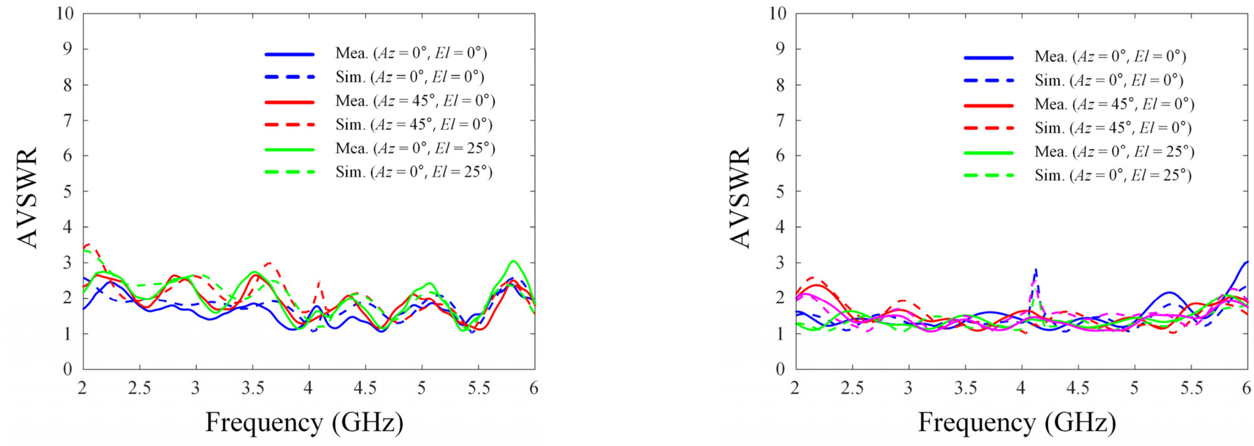


(a) (b)

Fig. 7. Measured and simulated AVSWR of the proposed array antenna: (a) Port 1 (the edge element) and (b) Port 6 (center port).

*n* are the index numbers of column and row elements ($M$ = 1, 2, 3…, and $N$ = 2, 4, 6 …). Fig. 7 shows the AVSWR results at steering angles (*Az*, *El*) of (0°, 0°), (45°, 0°), and (0°, 25°) for Port 1 (the edge element) and Port 6 (the center element). The measured and simulated AVSWRs for Port 1 are below 2.74:1 and 2.99:1 from 2.5 GHz to 5.5 GHz. The peak measured and simulated AVSWRs for Port 6 are 2.85 and 2.88, respectively, and these results agree well with each other. In addition, we obtain the array mismatch efficiency of the proposed array antenna as a figure of merit to evaluate the array performance for the high-power jammers using Eq. (6) [13].

$$eff = \left( I - \sum_{i=1}^{I} |\Gamma_i(Az, El)|^2 \right) / I. \quad (6)$$

Fig. 8 illustrates the measured and simulated array mismatch efficiency of the proposed array antenna at steering angles according to the frequency. The measured averaged array mismatch efficiencies over the entire frequency range are 91.3% (*Az* = 0°, *El* = 0°), 87.2% (*Az* = 45°, *El* = 0°), and 90.9% (*Az* = 0°, *El* = 25°), and those of the simulations are 93.6%, 90.4%, and 93.4%, respectively.

*3. Radiation Performance*

The AEPs for all ports of the proposed array are measured in an anechoic chamber to obtain the array radiation performance. The array gain is calculated using the AEPs of all ports based on Eq. (7) [14, 15]:

$$G_{array}(Az, El) = \frac{\sum_{i=1}^{I} \overline{w_i} \overline{g_i}(Az, El)}{\sqrt{\sum_{i=1}^{I} |w_i|^2}}, \quad (7)$$

where $g_i$ is a complex AEP vector of the *i*-th port, and $w_i$ is a complex weighting vector of the *i*-th port. Fig. 9 shows comparisons of the measured, simulated, and theoretical array gains in the bore-sight direction. The theoretical result is calculated as $4\pi A/\lambda^2$, where $A$ is the aperture area of the proposed array (in this case, 179 cm$^2$). All the results agree well with each other, and the measured array gain is above 9.5 dBi from 2 GHz to 6 GHz. To

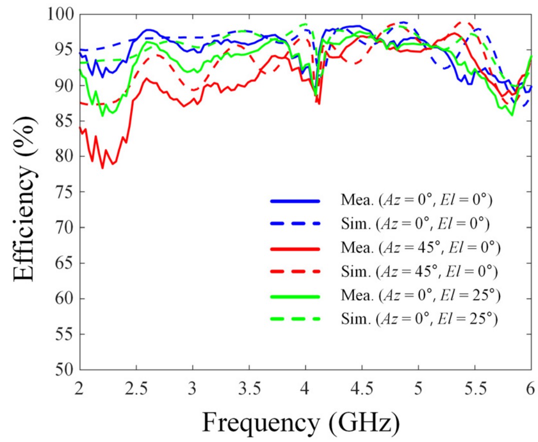


Fig. 8. Measured and simulated array mismatch efficiency of the proposed array antenna.

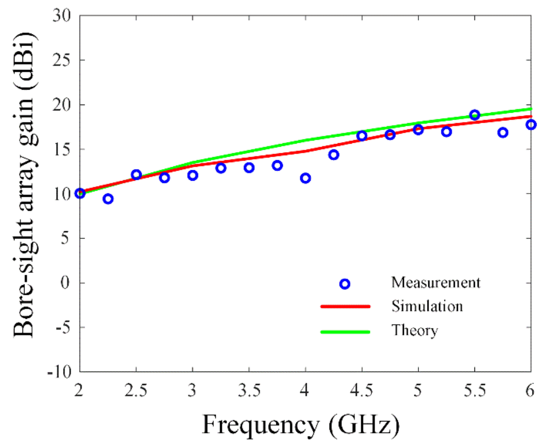


Fig. 9. Measured and simulated boresight gains of the proposed array antenna with theoretical results.

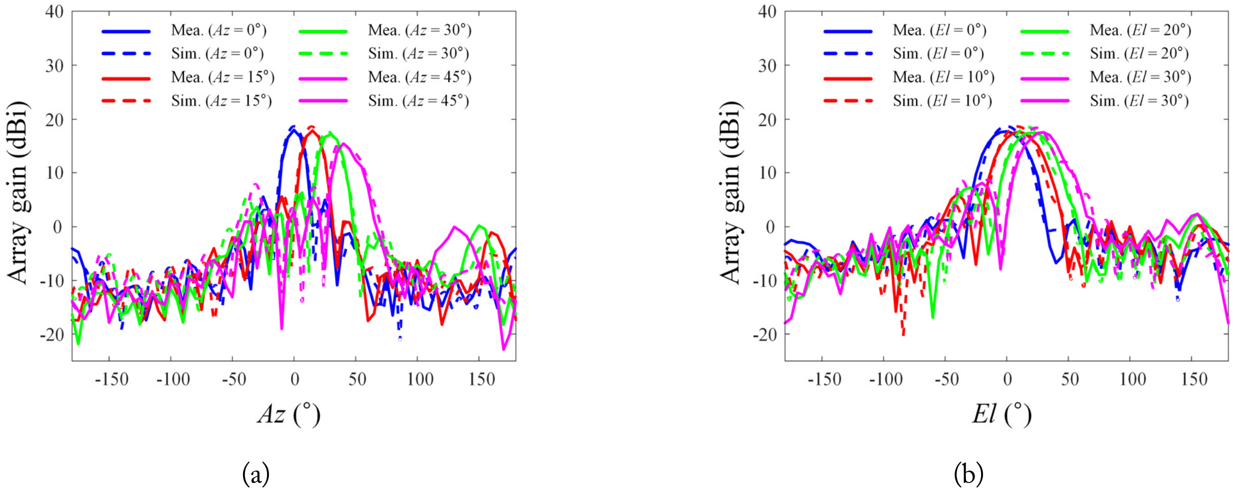


Fig. 10. Measured and simulated array radiation patterns according to beam-steering angles at 6 GHz: (a) E-plane and (b) H-plane.

Table 2. Comparison of the proposed antenna performance with that of existing references

| Study | Array gain at low-end frequency (dBi) | Number of array elements | Polarization | Bandwidth | Fabrication material |
|---|---|---|---|---|---|
| Yan et al. [6] | 7.3 | 8 × 8 | Dual | 9:1 | Metal |
| Kindt and Pickles [9] | 1.8[a)] | 8 × 8 | Dual | 12:1 | Metal |
| Zhang et al. [16] | 1.4[a)] | 1 × 26 | Dual | 5:1 | PCB |
| Zhong et al. [17] | 5 | 11 × 11 | Dual | 9:1 | PCB |
| Logan et al. [18] | 9.3[a)] | 19 × 19 | Single | 10:1 | PCB |
| Tzanidis et al. [19] | 2 | 7 × 7 | Single | 3:1 | PCB |
| Proposed | 10 | 4 × 4 | Dual-slant | 3:1 | Metal |

[a)]Estimated array gain from an element gain.

examine the beam steering performance, the complex weighting vector $w_i$ for each port is obtained at a high-end frequency of 6 GHz in accordance with the steering angle in the azimuth and elevation directions. Fig. 10 shows the beam steering performances along the E- and H-planes according to the steering azimuthal (*Az* = 0°, 15°, 30°, 45°) and elevational (*El* = 0°, 10°, 20°, 30°) angles at 6 GHz. The measured peak side lobe levels along the azimuth and elevation directions are 10.2 and 10.7 dB, respectively. The steered beam patterns can maintain high gain properties without the existence of grating lobes. The proposed array antenna performances are compared with previous works, as shown in Table 2 [6, 9, 16–19], for further explanation.

## IV. Conclusion

In this paper, we proposed the all-metal Vivaldi array antenna with dual-slant polarization for high-power jammer systems. The single Vivaldi element of the proposed array was composed of radiating flares and an inner cavity. The Vivaldi array element parameters were optimized using the periodic structure at the bore-sight direction to achieve broad frequency band characteristics. The maximum AVSWRs of the proposed array element were below 3:1 from 2 GHz to 6 GHz at steering angles (*Az*, *El*) of (0°, 0°) and (45°, 0°). It was expanded to a 4 × 4 array antenna with dual-slant polarizations in consideration of the grating lobes. The measured AVSWRs at Port 1and Port 6 were below 2.74:1 and 2.85:1, respectively, in the frequency range of 2.5–5.5 GHz, and the measured array gain was above 9.5 dBi from 2 GHz to 6 GHz. The results demonstrated that the proposed all-metal array antenna is suitable for high-power jammers due to its high gain and high durability.

This work was supported by the Agency for Defense Development Grant funded by the Korean government (No. 912758101).

## References

[1] J. Y. Deng, R. Cao, D. Sun, Y. Zhang, and L. X. Guo, "Bandwidth enhancement of an antipodal Vivaldi antenna facilitated by double-ridged substrate-integrated waveguide," *IEEE Transactions on Antennas and Propagation*, vol.

68, no. 12, pp. 8192-8196, 2020. https://doi.org/10.1109/TAP.2020.2997474

[2] K. Anim and Y. B. Jung, "Shortened log-periodic dipole antenna using printed dual-band dipole elements," *IEEE Transactions on Antennas and Propagation*, vol. 66, no. 12, pp. 6762-6771, 2018. https://doi.org/10.1109/TAP.2018.2874710

[3] J. Liu, S. Zhong, and K. P. Esselle, "A printed elliptical monopole antenna with modified feeding structure for bandwidth enhancement," *IEEE Transactions on Antennas and Propagation*, vol. 59, no. 2, pp. 667-670, 2011. https://doi.org/10.1109/TAP.2010.2096398

[4] B. R. Shookooh, A. Monajati, and H. Khodabakhshi, "Theory, design, and implementation of a new family of ultra-wideband metamaterial microstrip array antennas based on fractal and Fibonacci geometric patterns," *Journal of Electromagnetic Engineering and Science*, vol. 20, no. 1, pp. 53-63, 2020. https://doi.org/10.26866/jees.2020.20.1.53

[5] H. Kahkonen, J. Ala-Laurinaho, and V. Viikari, "Dual-polarized Ka-band Vivaldi antenna array," *IEEE Transactions on Antennas and Propagation*, vol. 68, no. 4, pp. 2675-2683, 2020. https://doi.org/10.1109/TAP.2019.2948561

[6] J. B. Yan, S. Gogineni, B. Camps-Raga, and J. Brozena, "A dual-polarized 2–18-GHz Vivaldi array for airborne radar measurements of snow," *IEEE Transactions on Antennas and Propagation*, vol. 64, no. 2, pp. 781-785, 2016. https://doi.org/10.1109/TAP.2015.2506734

[7] H. Holter, "Dual-polarized broadband array antenna with BOR-elements, mechanical design and measurements," *IEEE Transactions on Antennas and Propagation*, vol. 55, no. 2, pp. 305-312, 2007. https://doi.org/10.1109/TAP.2006.886557

[8] S. Hwang, B. Lee, D. H. Kim, and J. Y. Park, "Design of S-band phased array antenna with high isolation using broadside coupled split ring resonator," *Journal of Electromagnetic Engineering and Science*, vol. 18, no. 2, pp. 108-116, 2018. https://doi.org/10.26866/jees.2018.18.2.108

[9] R. W. Kindt and W. R. Pickles, "Ultrawideband all-metal flared-notch array radiator," *IEEE Transactions on Antennas and Propagation*, vol. 58, no. 11, pp. 3568-3575, 2010. https://doi.org/10.1109/TAP.2010.2071360

[10] G. F. Masters and S. F. Gregson, "Coordinate system plotting for antenna measurements," in *Proceedings of the Annual Symposium of the Antenna Measurement Techniques Association (AMTA)*, St. Louis, MO, USA, 2007.

[11] E. Sharp, "triangular arrangement of planar-array elements that reduces the number needed," *IRE Transactions on Antennas and Propagation*, vol. 9, no. 2, pp. 126-129, 1961. https://doi.org/10.1109/TAP.1961.1144967

[12] C. H. Liang, L. Li, and X. J. Dang, "Inequality condition for grating lobes of planar phased array," *Progress In Electromagnetics Research B*, vol. 4, pp. 101-113, 2008. https://doi.org/10.2528/PIERB07121901

[13] E. G. Tianang, M. A. Elmansouri, and D. S. Filipovic, "Ultra-wideband lossless cavity-backed Vivaldi antenna," *IEEE Transactions on Antennas and Propagation*, vol. 66, no. 1, pp. 115-124, 2018. https://doi.org/10.1109/TAP.2017.2775286

[14] A. K. Bhattacharyya, *Phased Array Antennas*. Hoboken, NJ: John Wiley & Sons, 2006.

[15] D. F. Kelley and W. L. Stutzman, "Array antenna pattern modeling methods that include mutual coupling effects," *IEEE Transactions on Antennas and Propagation*, vol. 41, no. 12, pp. 1625-1632, 1993. https://doi.org/10.1109/8.273305

[16] H. Zhang, S. Yang, Y. Chen, J. Guo, and Z. Nie, "Wideband dual-polarized linear array of tightly coupled elements," *IEEE Transactions on Antennas and Propagation*, vol. 66, no. 1, pp. 476-480, 2018. https://doi.org/10.1109/TAP.2017.2776959

[17] J. Zhong, A. Johnson, E. A. Alwan, and J. L. Volakis, "Dual-linear polarized phased array with 9:1 bandwidth and 60° scanning off broadside," *IEEE Transactions on Antennas and Propagation*, vol. 67, no. 3, pp. 1996-2001, 2019. https://doi.org/10.1109/TAP.2019.2891607

[18] J. T. Logan, R. W. Kindt, and M. N. Vouvakis, "A 1.2–12 GHz sliced notch antenna array," *IEEE Transactions on Antennas and Propagation*, vol. 66, no. 4, pp. 1818-1826, 2018. https://doi.org/10.1109/TAP.2018.2809476

[19] I. Tzanidis, K. Sertel, and J. L. Volakis, "UWB low-profile tightly coupled dipole array with integrated balun and edge terminations," *IEEE Transactions on Antennas and Propagation*, vol. 61, no. 6, pp. 3017-3025, 2013. https://doi.org/10.1109/TAP.2013.2250232

## Tae Heung Lim

https://orcid.org/0000-0001-7968-1272

received the B.S., M.S., and Ph.D. degrees in electronic and electrical engineering from Hongik University, Seoul, South Korea, in 2016, 2018, and 2022, respectively. He was a Postdoctoral Researcher in Ulsan National Institute of Science and Technology (UNIST) in 2022. He was a senior researcher with the Agency for Defense Development, Daejon, South Korea in 2023. He is currently an assistant professor with the School of Electronic Engineering, Kumoh National Institute of Technology, Gumi, South Korea. His research interests include space surveillance radar, 6G system antennas, sea-based radar, high-power array antennas, adaptive beamforming, and wave propagations for radar applications.

## Seulgi Park

https://orcid.org/0000-0003-0035-6667

received his B.S. and M.S. degrees in electrical engineering from Hongik University in 2006 and 2008. respectively. He worked at the Electronic Warfare Research Center of LIG Nex1 corporation from 2008 to 2013, and then from 2013 to 2016, he worked at the DMC Research Center of Samsung Electronics Corporation. Since January 2017, he has worked as a chief engineer in the tactical communication system team of Hanwha Systems. His major research fields include electronic warfare transmission/reception antennas, electronic warfare systems, and tactical communication systems.

## Cheol-Soo Lee

https://orcid.org/0000-0003-2135-5962

received his B.S. and M.S degrees in Electronic Engineering from Ajou University, Suwon, Korea, in 1990 and 1992, respectively, and his Ph.D. degree in Radio Science and Engineering from Chungnam National University, Daejeon, Korea, in 2016. Since 1992, he has been a chief principal researcher at the Agency for Defense Development, Daejeon, Korea. From 2013 to 2014, he was with the Department of Electrical and Computer Engineering, Air Force Academy, Colorado Springs, CO, USA, as a visiting scientist. His research interests include the design of wideband high-power transmitters and broadband phased array antennas as well as modeling and simulations of electronic warfare systems.

## Joo-Rae Park

https://orcid.org/0009-0000-7192-6490

received his B.S. and M.S degrees in Electronic Engineering from Chungnam National University, Daejeon, Korea, in 1991 and 1993, respectively, and his Ph.D. degree in Radio Science and Engineering from Chungnam National University, Daejeon, Korea in 2015. Since 1993, he has been a chief principal researcher at the Agency for Defense Development, Daejeon, Korea. His research interests include the design of wideband high-power transmitters and broadband wide-angle beamforming devices as well as modeling and simulations of electronic warfare systems.

## Hosung Choo

https://orcid.org/0000-0002-8409-6964

received his B.S. degree in radio science and engineering from Hanyang University in Seoul in 1998, and his M.S. degree and Ph.D. in electrical and computer engineering from the University of Texas at Austin, in 2000 and 2003, respectively. In September 2003, he joined the School of Electronic and Electrical Engineering, Hongik University, Seoul, Korea, where he is currently a full-time professor. His principal areas of research are the use of the optimization algorithm in developing antennas and microwave absorbers. His studies include the design of small antennas for wireless communications, reader and tag antennas for RFID, and on-glass and conformal antennas for vehicles and aircraft.